한국수소 및 신에너지학회 논문집(2009. 12), 제20권 제6호
Trans. of the Korean Hydrogen and New Energy Society(2009. 12), Vol. 20, No. 6, pp. 455~463

고체산화물 연료전지 금속연결재용 STS 444의 코발트 보호막 산화 특성

홍종은*,, 임탁형*, 이승복*, 유영성***, 송락현*†, 신동열*, 이덕열****

*한국에너지기술연구원 신재생에너지연구부, **고려대학교 신소재공학과, ***한국전력연구원 전략기술연구소

Oxidation Properties of Cobalt Protective Coatings on STS 444 of Metallic Interconnects for Solid Oxide Fuel Cells

JONGEUN HONG*,, TAKHYUNG LIM*, SEUNGBOK LEE*, YOUNGSUNG YOO***, RAKHYUN SONG*†, DONGRYUL SHIN*, DOKYOL LEE****

**Fuel Cell Research Center, New and Renewable Energy Research Division, Korea Institute of Energy Research, 71-2, Jang-dong, Yuseong-gu, Daejeon, Korea*
***Department of Materials Science and Engineering, Korea Univ., 5-1 Anam-dong, Seongbuk-gu, Seoul, Korea*
****Strategic Technology Laboratory, Korea Electric Power Research Institute, Korea Electric Power Corporation, Daejon, Korea*

ABSTRACT

코발트 보호막 코팅이 적용된 페라이트계 스테인리스 스틸인 STS 430과 STS 444 소재에 대해 고체산화물 연료전지용 금속연결재로서의 고온 산화 특성에 대해 살펴보았다. 코발트 코팅층은 800℃ 고온 산화 후 코발트 산화물 및 Co_2CrO_4, $CoCr_2O_4$, $CoCrFeO_4$ 등과 같은 코발트가 함유된 스피넬 상을 형성하였다. 또한 페라이트계 스테인리스 스틸과 코발트 코팅의 계면에서 크롬과 철이 함유된 치밀한 산화층을 형성하여 금속연결재 표면의 스케일 성장속도를 감소시키고 금속연결재 내에 함유된 크롬의 외부 확산을 효과적으로 억제하였다. 한편 STS 430은 고온 산화 후 표면에 형성된 스케일 하부에 SiO_2와 같은 내부 산화물이 형성된 반면 STS 444는 표면 스케일 이외에 다른 내부 산화물은 확인되지 않았으며 고온에서의 면저항 측정 결과, 코발트가 코팅된 STS 444의 전기 전도성이 STS 430 보다 우수한 것으로 나타났다.

KEY WORDS : Solid oxide fuel cell(고체산화물 연료전지), Metallic interconnect(금속연결재), Ferritic stainless steel(페라이트 스테인리스 스틸), Protective layer(보호막), Cobalt coating(코발트 코팅), Electroplating(전기도금)

1. Introduction

Fuel cells directly convert the chemical energy of fossil fuels into electrical energy without com-

†Corresponding author : rhsong@kier.re.kr
[접수일 : 2009.10.6 수정일 : 2009.11.26 게재확정일 : 2009.12.15]

bustion or any mechanical process. Among the various types of fuel cells, solid oxide fuel cell (SOFC) is a high-energy power generation system operating at an elevated temperature higher than 1000℃[1]. Interconnects are an important component of SOFC stacks. They separate fuel and oxidant gases and also electrically connect the anodes and the cathodes of the adjacent fuel cells in stacks. Therefore, SOFC interconnects must have a high temperature oxidation resistance in both oxidizing and reducing atmospheres and a high electrical conductivity. Ceramic and metallic materials are used as interconnects for SOFC applications[2]. Since the decrease of the operating temperature of SOFCs enables metallic interconnects to replace ceramic interconnects, many studies have been recently focused on discovering appropriate materials for metallic interconnects, due to advantages such as high electrical and thermal conductivities, low material cost, easy fabrication, and mechanical strength. Fe-Cr alloys of ferritic stainless steel containing chromium content higher than 16 wt. % are especially considered as promising materials. They represent a similar thermal expansion coefficient (TEC) of 12×10^{-6} compared to that of yttria-stabilized zirconia (YSZ), electrolyte materials[3]. However, the high temperature oxidation is one of the crucial problems in ferritic stainless steels due to the formation of an oxide scale of chromia (Cr_2O_3). The scale increases the resistance of the system so that it deteriorates the performance and long term stability of the SOFC stacks. In addition, the chromium poisoning occurred by the chromium diffusion from the oxide scale into the YSZ electrolyte in the cathode side also decreases the power density of the system[1,4,5].

In order to reduce the difficulties, various surface coatings have been investigated, which are electrically conductive, relatively compact, and chemically compatible and also prevent the migration of chromium into the cathodes.

Perovskites of (La, Sr)MnO_3[6,7] and spinels of (Mn, Cr)$_3O_4$[8] or (Mn, Co)$_3O_4$[9] are reported to be promising materials for the protective coating of metallic interconnects. The protective coatings are effective to decrease oxidation kinetics and improve electrical properties of SOFC metallic interconnects at high temperatures. It is also noted that a $(Mn_{1.5}Co_{1.5})O_4$ spinel layer is successful to suppress chromium outward diffusion[8]. In addition to perovskites and spinels, some studies based on a metallic coating of a transition element selected from Co, Mn, Ni, Cu and Fe have been reported. Badwal et al.[10] reported oxide coatings including at least one metal, M, of the transition elements. A M-Cr spinel layer was created between the metallic substrate containing chromium and the coating layer, resulting in a reaction between the coating layer and the surface oxide scale formed on the substrate. Stanislowski et al.[11] reported that metallic coatings of Co, Ni, and Cu and their oxides effectively inhibited the growth rate of the scale. Also, chromium migration could be suppressed by more than 99%. Zahid et al.[12] fabricated $MnCo_2O_4$ layers with Co_3O_4 coating by a wet powder spraying on the surface of Crofer22 APU. After 1000 h of oxidation, a scale formed at the interface between $MnCo_2O_4$ layer and $MnCr_2O_4$ sub-layer on Crofer22 APU was stable. Liang et al.[13] examined electrical and thermal properties of various spinel oxides. They observed that cobalt containing spinels represented higher electrical conductivities than that of Cr_2O_3. In our previous study, STS 430 with a protective cobalt coating was examined as a metallic interconnect for SOFCs. It indicated an improved conductivity and chromium retention at a high temperature but it was obviously seen that an internal oxide of SiO_2 was formed below the surface

of STS 430 after oxidation in both the coated and uncoated STS 430. In addition, the surface scale of the uncoated STS 430 was peeled off after oxidation, which was induced by SiO_2 with a smaller thermal expansion coefficient compared to that of steel[14]. Therefore, it would affect not only the stability but also the electrical performance of SOFC stacks since SiO_2 being an insulating material, has a low conductivity. In this study, we intend to improve the electrical conductivity and to enhance the oxidation resistance by means of a protective coating on a ferritic stainless steel as the metallic interconnect for SOFCs. Therefore, we evaluate the oxidation property of STS 444 coated with cobalt. The protective cobalt coating is prepared by electroplating on STS 444 subsequently the electrical conductivity and oxidation properties are investigated in comparison to STS 430 at 800℃ in air.

2. Experimental

2.1 Preparation of protective coating

Commercial ferritic stainless steels, STS 430 and 444, are used as metallic interconnect materials for SOFC applications. The typical composition of the steels are listed in Table 1. STS 444 contains a higher chromium concentration than that of STS 430. Samples of STS 430 and 444 have an area of 10 × 10 mm^2 and 3 mm and 1 mm thickness, respectively. Each coupon is mechanically polished with SiC paper to # 2000 grit. For degreasing, each piece is ultrasonically cleaned in 0.1 M sodium hydroxide (NaOH) solution and then in acetone, respectively and subsequently rinsed in distilled water. The cobalt coating layer is prepared by electroplating. Each sample is pickled in 10% hydrochloric acid (HCl) for 1 min to remove the surface oxide scale on the stainless steel just before electroplating, followed by rinsing in distilled water. A cobalt plate with dimensions of 15 × 15 × 1 mm and the coupon of the stainless steel are used as anode and cathode in electroplating, respectively. An electroplating solution is prepared by dissolving 1 M of $CoSO_4 \cdot 7H_2O$, 0.3 M of $CoCl_2 \cdot 6H_2O$, and 0.2 M of H_3BO_3 in 0.5 L of distilled water which was degassed by blowing N_2 gas for 6 h[15]. Cobalt is electroplated on the coupons at a current density of 50 $mAcm^{-2}$ using Digital Sourcemeter 2400 series (KIETHLEY) for 40~70 min in the solution, resulting in a coating of ca. 25~65 ㎛ thickness. After electroplating, each specimen is rinsed with distilled water (heated to 70~80℃) and ethanol, respectively, followed by drying at 200℃ in air. The coated substrate is heat-treated at 800℃ for 10 h in a reducing atmosphere (10% H_2 and N_2 gas) to reinforce the adhesion between cobalt coating layer and stainless steel before the high temperature oxidation.

2.2 ASR measurement

The area specific resistance (ASR) is measured for 800 h at 800℃ in air to evaluate electrical conductivities of cobalt coated and uncoated steels.

Table 1 Typical chemical composition (wt. %) of STS 430 and STS 444

	Cr	Mn	Mo	Si	Al	Ni	Ti	Nb	P	S	C	etc
STS 430	16-18	≤ 1.0	-	≤ 0.75	≤ 0.2	≤ 0.6	-		≤ 0.04	≤ 0.03	≤ 0.12	
STS 444	17-20	≤ 1.0	1.75-2.5	≤ 1.0	-	≤ 0.6	Ti, Nb 8x(C+N)-0.8		≤ 0.04	≤ 0.03	≤ 0.025	N (≤ 0.025)

The ASR test is conducted by a four-probe method. Platinum mesh and platinum wires are used for contact media and current leads, respectively. A dead load of 4×10^4 Pa is applied on the platinum mesh during the ASR test. Each platinum mesh has two welded platinum leads. A constant current density of 500 $mAcm^{-2}$ is supplied by Digital Sourcemeter 2400 series (KIETHLEY) while the voltage is measured.

2.3 Chemical characterizations

Electroplated samples are characterized by X-ray diffraction (XRD) to confirm phase transformations of cobalt coatings along with the oxidation time at 800℃. Scanning electron microscopy (SEM) and energy dispersive spectroscopy (EDS) are used to identify the cross-section, surface morphology, and elemental distributions of the cobalt coatings and interconnects.

3. Results and discussion

3.1 X-ray diffraction analysis

Cobalt coatings are characterized by XRD for the samples of as-deposited and after oxidation for 1 h and 320 h, respectively, at 800℃ in air (Fig. 1). The as-deposited cobalt coating on STS 444 exhibits a pure cobalt phase with hexagonal structure (Fig. 1(a)). The cobalt coating is oxidized to CoO and $CoCo_2O_4$ after oxidation for 1 h. It can be seen that $CoCo_2O_4$ of cobalt oxide is confirmed after oxidation for 320 h indicating a complete oxidation of the cobalt coating. In addition, a few cobalt containing spinel phases are developed such as Co_2CrO_4, $CoCr_2O_4$, and $CoCrFeO_4$ after 320 h at 800℃ in air (Fig. 1(c)). Thus, cobalt coating layers are transformed into cobalt oxide and cobalt containing spinel phases after the long-term oxidation.

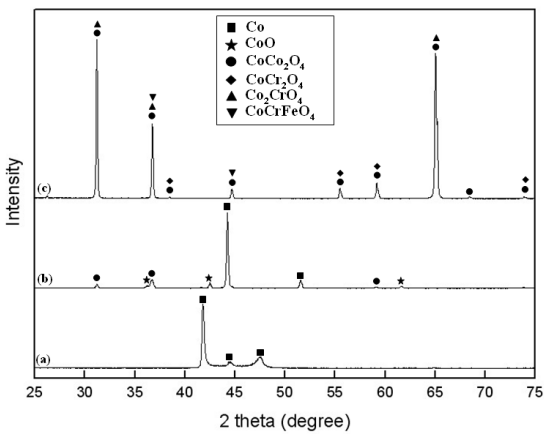

Fig. 1 XRD results of cobalt coatings on SUS 444; (a) as-deposited and (b) 1 h, and (c) 320 h oxidation at 800℃ in air.

3.2 Microstructure and phase analysis

The surface morphology and cross-section of cobalt coatings on STS 444 are investigated by scanning electron microscopy after oxidation in air. The cobalt-coated steel is heat-treated in 10% H_2 and N_2 gas in order to enhance the adherence between STS 444 and the cobalt coating prepared by electroplating before oxidation.

Fig. 2 shows surface images of uncoated and the cobalt-coated STS 444 after oxidation at 800℃ for 320 h. The surface morphology of the uncoated steel is coarse and porous with agglomerated particles. On the other hand, cobalt coated STS 444 reveals a uniform and smooth morphology compared to that of the uncoated stainless steel.

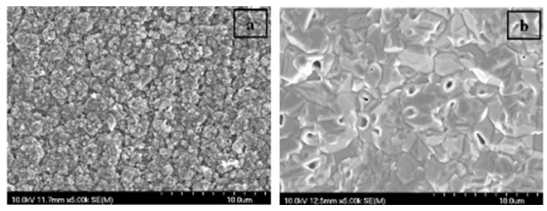

Fig. 2 Surface images of (a) uncoated and (b) cobalt coated US 444 after oxidation at 800℃ in air for 320 h.

Also, the cobalt coated surface indicates a dense surface with good adherence.

The SEM micrograph and elemental mapping of the cross-section of cobalt coated STS 444 after 1020 h are shown in Fig. 3. It can be seen that a dense layer of chromium oxide is thermally grown at the interface between STS 444 and the cobalt coating layer. The result of elemental mapping reveals no diffusion of chromium proceeded into the coating layer after the long-term oxidation in air.

Also, the result of EDS line scan indicates that a dense oxide scale containing Co, Fe, Cr-, and a small amount of Mn is formed at the interface between STS 444 and the cobalt coating as shown in Fig. 4. The oxide scale consists of cobalt containing spinel phases such as Co_2CrO_4, $CoCr_2O_4$, and $CoCrFeO_4$ which are confirmed by XRD analysis in Fig. 1. In addition, a small amount of Mn is detected in the dense scale as shown in Fig. 3 and 4. It is normally reported that a small amount of Mn contained in the ferritic stainless steel is transformed into $(MnCr)_3O_4$ oxide on top of the scale grown on the surface of the steel after high temperature oxidation. The $(MnC)r_3O_4$ oxide is also electrically conductive and reduces the oxidation rate of chromium containing stainless steels[16]. It can be obviously seen that chromium element rarely exists in the cobalt coating after oxidation for 1020 h due to the cobalt containing dense scale as shown in Fig. 4. A possible explanation for the chromium retention is that transition metals like Co, Ni, and Cu and their oxides are known to not only effectively reduce the growth rate of the scale but also prevent the chromium outward diffusion[11]. Thus, the chromium diffusion is effectively inhibited by the cobalt oxide layer, followed by the formation of a dense oxide scale thermally grown at the interface after high temperature oxidation.

The uncoated STS 444 has no spallation from the surface oxide after oxidation as shown in Fig. 2(a). In our previous work, an oxide scale developed on uncoated STS 430 was partially peeled off after long-term oxidation since the subscale of SiO_2

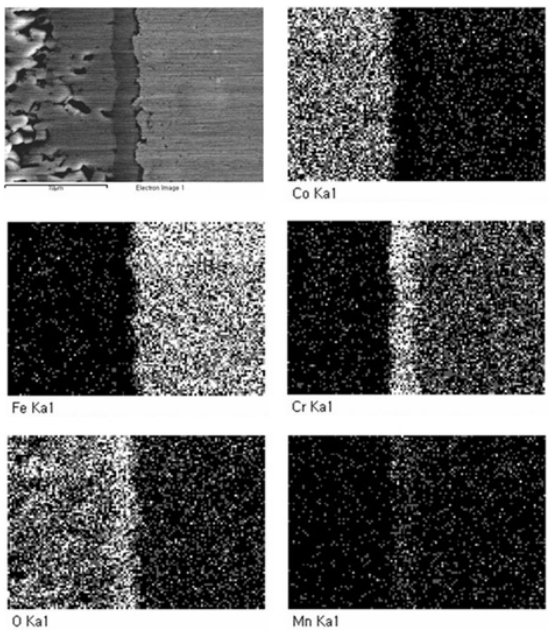

Fig. 3 Elemental mappings of the cross-section of cobalt coated SUS 444 after oxidation at 800℃ in air for 1020 h.

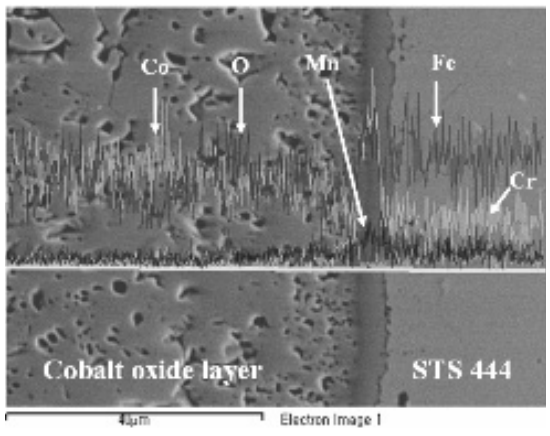

Fig. 4 The EDS line scan of the cross-section of cobalt coated STS 444 after oxidation for 1020 h.

generated below STS 430 surface caused the scale to spall off as shown in Fig. 3(a)[14]. Since SiO_2 of the subscale has a smaller thermal expansion coefficient compared to that of STS 430, it affects the deterioration of the scale adherence[5]. Therefore, it would increase a sensitivity for the delamination of the surface scale at a high temperature. However, the SEM image of a cross-section of the uncoated STS 444 indicates only a surface scale growth and no subscale below the scale after oxidation as shown in Fig. 5(b). Further experiment was conducted to define the surface oxide scale formed on the uncoated sample by EDS analysis as shown in Fig. 6. The scale is composed of mainly Cr, O, and a small amount of Mn, which seems to be the $(MnCr)_3O_4$ phase. In addition, minor elements of Nb and Al listed in Table 1 are confirmed. It is noted that not only a small amount of alloy element such as Ti, Mn, and Al is normally added to improve the oxidation resistance of metallic interconnect at a high temperature but also a tiny amount of La, Zr, Nb, and/or Mo element is exploited to decrease the oxidation rate[2,17]. Therefore, the minor elements could inhibit the formation of a subscale on the stainless steel since they influence the suppression of the subscale formation on STS 444, so that the scale adherence generated on the uncoated STS 444 is increased, subsequent to an improvement in the oxidation property compared to that of the uncoated STS 430 after long-term oxidation in air.

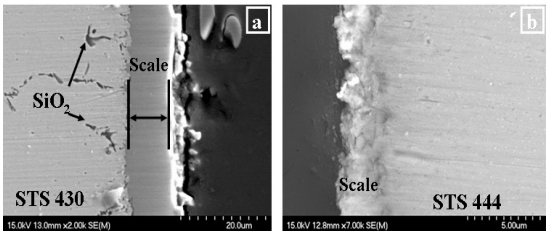

Fig. 5 SEM images of cross-sections of (a) uncoated STS 430[14] and (b) uncoated STS 444 of Fig. 2 (a) after oxidation.

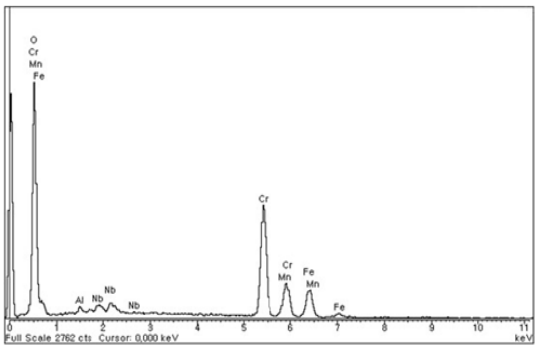

Fig. 6 EDS analysis of the surface of uncoated STS 444 as shown in Fig. 2 (a).

3.3 Electrical conductivity

The area specific resistance is measured to examine electrical conductivities of cobalt coated STS 430 and 444, respectively, after oxidation at 800℃. A constant current density of 500 $mAcm^{-2}$ is supplied while the voltage is measured during the measurement. Fig. 7 shows the ASR values of coated STS 430 and 444 during heating at 800℃ in air as a function of time. It was reported in our previous study that cobalt coated STS 430 had a

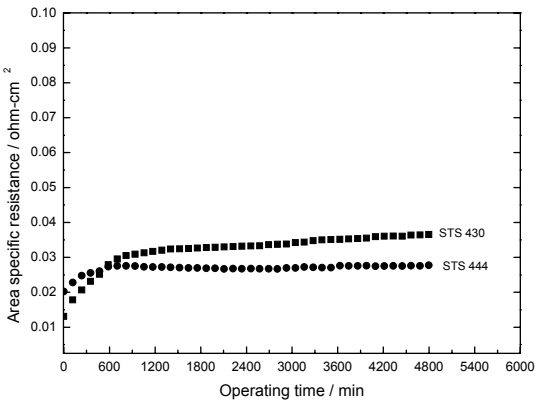

Fig. 7 ASR values for STS 430 and 444 coated with cobalt after oxidation at 800℃ for 800 h.

reduced ASR value in comparison with that of uncoated sample after oxidation[14]. In this result, the ASR of STS 444 is lower than that of STS 430 at 800℃ for 800 h. In addition, the ASR of STS 430 indicates a rapid increment of resistance during initial stage and then exhibits a linearly continuous increment, whereas STS 444 reveals a higher resistance within 100 h but gradually increases at a relatively lower rate than that of STS 430. After oxidation for 800 h, the ASR value of cobalt coated 444 is 0.0277 Ωcm^2 lower than 0.0365 Ωcm^2 of STS 430 and indicates a stable increase. A possible explanation for the ASR difference between the steels is that the internal oxide of SiO_2 in STS 430 could induce the electrical conductivity to decrease since it is an insulator[14]. However, STS 444 has no internal oxide after oxidation. Also, the improvement of the electrical conductivity for coated stainless steels at a high temperature is attributed to the decrease in the resistance of Cr_2O_3. Electrical holes in the scale are formed by doping Co^{2+} from the coating or Fe^{2+} from the steel into the scale so that the increment of the hole density results in an increase in the dimension of the path which enables the electron to move at a high temperature[13,18]. Also, cobalt oxide and cobalt containing spinels developed at the interface between the cobalt coating and STS 444 have a higher electrical conductivity than the oxide scale of Cr_2O_3 formed on the uncoated sample[13]. Therefore, STS 444 represents a lower electrical resistance than STS 430 and the protective cobalt coating on STS 444 improves the electrical conductivity of metallic interconnects for SOFC applications at high temperatures.

4. Conclusion

Cobalt coatings were prepared by electroplating on STS 430 and 444 of metallic interconnect as a protective coating. The cobalt coating was transformed into cobalt oxide and cobalt containing spinel phases such as Co_2CrO_4, $CoCr_2O_4$, and $CoCrFeO_4$ after oxidation at 800℃ in air. Also, a dense layer containing Co, Fe, and Cr was thermally grown at the interface between the stainless steel and cobalt coating after the long-term oxidation, resulted in the cobalt containing spinel phases. In addition, the dense layer not only efficiently prevented a chromium migration into cobalt coatings but also improved an electrical conductivity of metallic interconnect, due to higher conductivities of cobalt oxide and cobalt containing spinels compared to that of Cr_2O_3. Compared with oxidation properties of cobalt coated STS 430 and 444, STS 444 transformed no subscale and indicated an improved electrical conductivity, since a small amount of element such as Mn, Nb, and Al induced an increment in the oxidation resistance. Also, it was supposed that SiO_2 of the internal oxide affects the electrical conductivity of the metallic interconnect after high temperature oxidation. Thus, cobalt-coated STS 444 represented a possibility as a promising metallic interconnect material for SOFC applications.

Acknowledgement

This work was supported by New & Renewable Energy R&D program (2006-N-FC12-P-04) under the Ministry of Knowledge Economy (MKE).

References

1) S. C. Singhal, “Solid Oxide Fuel Cells for Stationary, Mobile, and Military Applications”, Solid State Ionics, Vol. 152-153, 2003, pp. 405-410.
2) K. Hilpert, W. J. Quadakkers, and L. Singheiser,

"Handbook of Fuel Cells, Fundamentals Technology and Applications, Chap. 74-Interconnects", John Wiley & Sons, Chichester, Vol. 4, 2003.
3) Y. Matsuzaki and I. Yasuda, "Electrochemical Properties of a SOFC Cathode in Contact with a Chromium-containing Alloy Separator", Solid State Ionics, Vol. 132, 2000, pp. 271-278.
4) K. Hilpert, D. Das, M. Miller, D. H. Peck, and R. Weiß, "Chromium Vapor Species over Solid Oxide Fuel Cell Interconnect Materials and Their Potential for Degradation Processes", J. Electrochem. Soc., Vol. 143, 1996, pp. 3642-3647.
5) P. Huczkowski, N. Christiansen, V. Shemet, L.Niewolak, J. P. Abellan, L. Singheiser, and W. J. Quadakkers, "Growth Mechanisms and Electrical Conductivity of Oxide Scales on Ferritic Steels Proposed as Interconnect Materials for SOFCs", Fuel Cells, Vol. 6, 2006, pp. 93-99.
6) H. W. Nie, T. Wen, and H. Y. Tu, "Protection Coatings for Planar Solid Oxide Fuel Cell Interconnect prepared by Plasma Spraying", Mater. Res. Bull., Vol. 38, 2003, pp. 1531-1536.
7) J. H. Kim, R. H. Song, and S. H. Hyun, "Effect of Slurry-coated LaSrMnO3 on the Electrical Property of Fe–Cr Alloy for Metallic Interconnect of SOFC", Solid State Ionics, Vol. 174, 2004, pp. 185-191.
8) Z. Yang, G. G. Xia, S. P. Simner, and J. W. Stevenson, "Thermal Growth and Performance of Manganese Cobaltite Spinel Protection Layers on Ferritic Stainless Steel SOFC Interconnects", J. Electrochem. Soc., Vol. 152, 2005, pp. A1896-A1901.
9) Z. Yang, G. G. Xia, X. H. Li, and J. W. Stevenson, "(Mn,Co)3O4 Spinel Coatings on Ferritic Stainless Steels for SOFC Interconnect Applications", Int. J. Hydrogen Energy, Vol. 32, 2007, pp. 3648-3654.
10) S. P. S. Badwal, R. Deller, K. Foger, Y. Ramprakash, and J. P. Zhang, "Interaction Between Chromia Forming Alloy Interconnects and Air Electrode of Solid Oxide Fuel-Cells", Solid State Ionics, Vol. 99, 1997, pp. 297-310.
11) M. Stanislowski, J. Froitzheim, L. Niewolak, W. J. Quadakkers, K. Hilpert, T. Markus, and L. Shingheiser, "Reduction of Chromium Vaporization from SOFC Interconnectors by Highly Effective Coatings", J. Power Sources, Vol. 164, 2007, pp. 578-589.
12) M. Zahid, F. Tietz, D. Sebold, H. P. Buchkremer, "Reactive Coatings against Chromium Evaporation in Solid Oxide Fuel Cells", In: Mogensen M, editor. Proceedings of third European SOFC forum, European solid oxide fuel cell forum, Switzerland. 2004. pp. 820.
13) H. Ling and A. Petric, "Electrical and Thermal Properties of Spinels", in Solid Oxide Fuel Cells (SOFC IX), J. Mizusaki and S. C. Singhal (Eds), The Electrochemical Society Proceedings Series, Pennington, NJ, PV 2005-07, 2005, pp. 1866-1873.
14) J. E. Hong, T. H. Lim, R. H. Song, S. B. Lee, D. R. Shin, Y. S. Yoo, D. Y. Lee, "Effects of Cobalt Protective Coating Prepared by DC Electroplating on Ferritic Stainless Steel for SOFC Interconnect", Trans. of the Korean Society of Hydrogen Energy, Vol. 20, No. 2, 2009, pp. 116-124.
15) M. Schlesinger and M. Paunovic, "Modern Electroplating", 4th ed., John Wiley & Sons, USA, 2000.
16) Z. Yang, J. S. Hardy, M. S. Walker, G. Xia, S. P. Simner, and J. W. Stevenson, "Structure and Conductivity of Thermally Grown Scales on Ferritic Fe-Cr-Mn Steel for SOFC Interconnet Applications", J. Electrochem. Soc. vol. 151, 2004, pp. 1825-1831.

17) K. Honegger, A. Plas, R. Diethelm, W. Glatz, “Evaluation of Ferritic Steel Interconnects for SOFC Stacks”, in Solid Oxide Fuel Cells (SOFC VII), H. Yokokawa and S. C. Singhal (Eds), The Electrochemical Society Proceedings Series, Pennington, NJ, PV 2001-16, 2001, pp. 803-810.

18) Y. Larring and T. Norby, “Spinel and Perovskite Functional Layers between Plansee Metallic Interconnect (Cr-5wt% Fe-1wt% Y2O3) and Ceramic (La0.85Sr0.15)0.91MnO3 Cathode Materials for Solid Oxide Fuel Cells”, J. Electrochem. Soc., Vol. 147, 2000, pp. 3251-3256.